Carbohydrate Polymer Technologies and Applications 7 (2024) 100457

Contents lists available at ScienceDirect

Carbohydrate Polymer Technologies and Applications

journal homepage: www.sciencedirect.com/journal/carbohydrate-polymer-technologies-and-applications

Synthesis and Characterization of Antimicrobial Bacterial Cellulose Crosslinked with Branched Polyethylenimine

Bentolhoda Heli [a], Georges R. Younes [a], Kattin Arguindeguy [a,b], Abdellah Ajji [a,*]

[a] CREPEC, Département de Génie Chimique, Polytechnique Montréal, P.O. box 6079, Station Centre-Ville, Montréal, Québec H3C3A7, Canada
[b] Grenoble INP - Pagora, Université Grenoble Alpes, 461 rue de la Papeterie - CS 10065-38402 Saint-Martin d'Hères Cedex, France

ARTICLE INFO

Keywords:
Bacterial cellulose
Antimicrobial properties
Polyethylenimine
Crosslinking
Facemask

ABSTRACT

This study examines the development of composite bacterial cellulose (BC) sheets with antimicrobial properties for potential application in face masks. Branched polyethylenimine (PEI) is employed as the antimicrobial agent, effective against both gram-positive and gram-negative bacteria. Various concentrations of PEI are crosslinked into BC via epichlorohydrin under moderate conditions. The thermal and morphological properties of dried BC-PEI samples are comprehensively characterized. Results reveal that introducing PEI via crosslinking minimally impacts the thermal stability of BC, without any discernible physical disruption. Nevertheless, BC-PEI matrices present lower water evaporation enthalpies than BC, based on dynamic scanning calorimetry, caused by alteration of hydrogen bonding interactions (amine groups versus hydroxyl groups). Moreover, dried BC-PEI samples exhibit an improved efficacy against gram-positive bacteria as compared to gram-negative bacteria; *S. aureus* and *P. aeruginosa*, respectively. Indeed, a 2.5% (wt/v% of Milli-Q water) PEI concentration completely inhibits the growth of *S. aureus* after 6 h, while a 7.5% PEI concentration achieves similar effects on *P. aeruginosa*. Despite the notable antibacterial efficacy of BC-PEI matrices, their antiviral efficacy is less pronounced. This difference in antibacterial and antiviral efficacies could be attributed to variations in microorganism characteristics, mechanisms of action, and structures of PEI.

1. Introduction

Respiratory infections, despite their historical context, remain a persistent concern that necessitates constant vigilance. They, especially the ones caused by both bacterial and viral agents, are of particular importance as they introduce intricate complexities to the domain of public health management. A recent example is the prevalence of coronaviruses as demonstrated by the Severe Acute Respiratory Syndrome Coronavirus 2 (SARS-CoV-2) which emphasizes the variety of respiratory ailments associated with the COVID-19 syndrome. Moreover, the co-infection of viral respiratory infections, such as influenza and COVID-19, with bacterial pathogens can worsen disease severity and increase mortality rates (Lansbury, Lim, Baskaran, & Lim, 2020; Li, Zhang, Ren, The Chinese Centers for Disease, & Prevention Etiology of Respiratory Infection Surveillance Study, 2021). In both bacterial and viral infections, the primary mode of transmission involves the inhalation of respiratory droplets generated through coughing, sneezing, and even normal respiration (Gao et al., 2021). While vaccines and definitive treatments of COVID-19 remain limited, governments around the world are reinforcing disease management strategies by establishing public health protocols to follow, including the use of masks and the practice of physical distancing. Amid the ongoing pandemic, the World Health Organization endorsed the use of masks as a means to mitigate viral transmission (Gope, Gope, & Gope, 2020). On the other hand, it is crucial to acknowledge that textile masks may exhibit compromised filtration efficiency, potentially resulting in viral accumulation. Consequently, there has been a significant focus on developing innovative materials that ensure both safety and efficacy within this context.

Recent efforts have explored the fabrication of antimicrobial face masks to reduce the risk of human contamination from infected aerosols (Pullangott, Kannan, Gayathri, Kiran, & Maliyekkal, 2021). Various antimicrobial agents, differing in nature and form, such as shellac/-copper nanoparticles (Kumar et al., 2020), silver nanoparticles (Chen et al., 2022), silver nanowires (Wu et al., 2022), quaternary ammonium compound nanoparticles (Xiong et al., 2020), and antibacterial polymers (Shanmugam et al., 2021) were incorporated into the mask matrices. Recently, polycationic polymers, including cationic polyethylenimine polymers (PEI), have gained attention due to their

* Corresponding author.
E-mail address: abdellah.ajji@polymtl.ca (A. Ajji).

https://doi.org/10.1016/j.carpta.2024.100457

Available online 8 February 2024
2666-8939/© 2024 The Authors. Published by Elsevier Ltd. This is an open access article under the CC BY-NC-ND license (http://creativecommons.org/licenses/by-nc-nd/4.0/).

selective antibacterial properties and the abundance of functional groups available for surface grafting. PEI is well-known in the field of biomedical applications as a versatile non-viral vector for nucleic acid delivery, which is owed to its high transfection efficiency (Pandey & Sawant, 2016). However, its toxicity remains a concern which is related to structural properties, such as molecular weight and linearity. Nevertheless, it is reported that PEI associated with nucleic acid exhibited less toxicity in comparison with the unbound and free PEI (Pandey & Sawant, 2016).

Despite these considerations, the antimicrobial properties of PEI have been demonstrated in both unmodified and modified forms while being covalently linked to other components. Research by Wiegnad group, for instance, assessed the impact of PEI on *Staphylococcus aureus* and *Escherichia coli* for dermal applications (Wiegand, Bauer, Hipler, & Fischer, 2013). They investigated linear and branched PEI variants with molecular weights ranging from 0.8 to 750 kDa. Their findings indicated that both types of PEI significantly inhibited bacterial growth, with a more noticeable effect on gram-positive bacteria. Additionally, variations in PEI molecular structure and molecular weight influenced its antibacterial efficacy and cytotoxicity, whereas the linear and branched PEIs with lower molecular weights revealed higher biocompatibility (Wiegand et al., 2013). Consequently, numerous studies have explored the modification of PEI, involving covalent grafting onto other components to enhance its effectiveness and biocompatibility. Examples include starch/chitosan/polyethylenimine blend films crosslinked by citric acid (Zhang, Han, Ben, Han, & Yin, 2023), mannose-modified polyethylenimine (Liu, Li, & Li, 2018), N, N-dodecyl, methyl-polyethylenimine (PMPEI) (Larson, Oh, Knipe, & Klibanov, 2013), cellulose-based hydrogel (Wahid et al., 2020), and PEI-functionalized Ag nanoparticles (Liu et al., 2014). PEI grafting onto surfaces has also been investigated to improve the biocidal and virucidal activity for various applications. PEI derivatives, such as N-hexylated-methylated high-molecular-weight polyethylenimine, have been grafted onto wools, nylon, and cotton to enhance the antimicrobial and antifungal properties of woven textiles (Lin, Qiu, Lewis, & Klibanov, 2003). Similarly, PEI has been immobilized on the surface of polypropylene microfiltration membranes (PPMMs) to improve their antifouling and antibacterial activity (Qiu, Zhao, Du, Hu, & Xu, 2017).

The high efficient antibacterial face masks are obtained from incorporating desired antimicrobial agents into porous sheets and fibrous matrices fabricated from diverse materials and techniques, including polypropylene (PP) (Kumar et al., 2020; Xiong et al., 2020), polyacrylonitrile (PAN) (Chen et al., 2022), and cellulose-based materials (Wu et al., 2022). In recent years, bacterial cellulose (BC) has caught researchers' attention as a filtering material for face masks due to its unique properties such as biodegradability, nanofibrous structure with high porosity, biocompatibility, flexibility, and mechanical strength (Jonsirivilai, Torgbo, & Sukyai, 2022; Żywicka et al., 2023). Moreover, BC's versatility is highlighted in its diverse applications in the biomedical field, including wound healing (Lin, Lien, Yeh, Yu, & Hsu, 2013), tissue engineering scaffolds (Raut, Asare, Syed Mohamed, Amadi, & Roy, 2023), drug delivery (Badshah et al., 2018), cosmetic formulations (Martins, Rocha, Dourado, & Gama, 2021), and sheet masks (Sharma, Mittal, Yadav, & Aggarwal, 2022; Stanislas et al., 2022). Its filtration capabilities, in addition to its compatibility with the human body, render it a promising candidate for face mask applications.

This study focuses on developing BC-PEI composites by covalently bonding the hydroxyl groups present in BC and the abundant amine groups (primary and secondary) in PEI through appropriate crosslinking techniques (Riva, Fiorati, & Punta, 2021). To create a stable BC-PEI, we utilized epichlorohydrin (EPI) as the crosslinker by conducting the reaction under moderate conditions with varying concentrations of a branched PEI. Upon completing this wet chemistry reaction, the samples were thoroughly dried. Unlike previous studies that primarily explored BC-PEI hydrogels in their hydrated form, our study aims to analyze the structural and thermal properties of the dried BC-PEI matrices. Additionally, we evaluated the bactericidal and virucidal of these dried BC-PEI sheets that are just partially moistened with phosphate-buffered saline (PBS) at pH 7.4 against *S. aureus* (gram-positive), *P. aeruginosa* (gram-negative), and human coronavirus 229E (ATCC® VR-740™) with varying contact times. Analyzing the BC-PEI samples in their dry state provides a deeper understanding of their stability and effectiveness in real-world applications where they are not fully hydrated.

2. Material and Methods

Bacterial cellulose (BC) was obtained from Nano Novin Polymer Co. (Iran, Gorgan). Branched polyethylenimine (PEI) (Average Mw ~25,000), Orange II sodium salt (4-(2-Hydroxy-1-naphthylazo) benzenesulfonic acid sodium salt), epichlorohydrin, beef extract powder, peptone powder, minimum essential medium eagle (EMEM), and fetal bovine serum (FBS) were all purchased from Sigma (Canada, ON). *Staphylococcus aureus* (*S. aureus*) (ATTC® 6538™), *Pseudomonas aeruginosa* (*P. aeruginosa*) (ATCC® 15442™), human coronavirus 229E (HcoV-229E) (ATCC® VR-740™), and human cell line MRC-5 (ATCC CCL-171™) were purchased from Cedarlane® (Canada, ON). D/E Neutralizing Broth, CRITERION™ Dehydrated Culture Media, and LB broth Miller (Luria-Bertani) were acquired from VWR™ (Canada, ON).

2.1. Preparation of BC Crosslinked PEI

BC sheet was received in the form of gel sheets immersed inside 1% acetic acid. First, the sheets were repeatedly washed with plenty of Milli-Q water to remove the acid residue. Then, they were dried out at room temperature by being sandwiched between filter papers and a Teflon sheet. Upon complete dryness, they were cut into pieces of 2×2 cm^2. The BC-PEI crosslinking procedure was adapted from the procedure reported previously by Wahid et al. (2020). Briefly, 0.2 g of cut BC was immersed into 10 ml of NaOH 2 M and 3 ml epichlorohydrin. The mixture was kept under vigorous stirring and at 45°C for 2 h. Then, 2 mL of PEI solution dissolved in Milli-Q water was added to the mixture while the temperature rose to 75°C. PEI concentrations were adjusted in Milli-Q water and varied from 2.5%, 5%, 7.5% and 10% (wt/v%). The reaction was finally terminated after 18 h by removing BC from the mixture and washing it repeatedly with Milli-Q water under vigorous stirring and at room temperature to remove all unbound reagents. The BC-crosslinked PEI pieces were dried in a similar manner as described above and then stored in a sealed container for further use.

The thickness of pristine BC and crosslinked BC-PEI samples was evaluated using ProGage Thickness Tester (Thwing-Albert Instrument Company, Berlin, Germany) and reported as an average of 12 different measurements on different samples.

2.2. Analytical Characterization of BC Crosslinked PEI

2.2.1. Colorimetric technique

The colorimetric method using Orange II was utilized to determine the quantity of PEI crosslinked to the surface of BC, as previously documented by Noel et al. (2013). Accordingly, individual BC samples and crosslinked BC-PEI pieces, each measuring 2×2 cm^2, were submerged in 5 mL of Orange II dye solution at 50°C and for 60 min. The dye solution, with a concentration of 14 mg/mL, was prepared in acidic water containing Milli-Q water with an adjusted pH of 3 using 1 M HCl. After that, the samples underwent multiple rinse cycles using acidic water (pH 3) to completely remove any unbound dye. Once thoroughly rinsed, the samples were air-dried at room temperature. The drystained samples were then placed in 5 ml of basic water (Milli-Q water adjusted to pH 12 using 1 M NaOH) and maintained at 65°C for 60 min. The solution containing the detached dye was then acidified by adding 2-5 μl of 12.3 M HCl to reach pH 3. The absorbance of this solution was subsequently measured at a wavelength of 484 nm by a spectrophotometer (SPECTRONIC™ 200 Spectrophotometer, Thermo Fisher Scientific Inc.).

Ultimately, the quantity of PEI was evaluated utilizing a pre-established calibrated linear curve correlating the measured absorbance with defined dye concentrations.

2.2.2. Fourier-transform infrared spectroscopy (FTIR-ATR)

The infrared spectra of BC, PEI, and BC-PEI crosslinked sample containing 10% (wt/v%) PEI were recorded by a Perkin Elmer 65 FTIR-ATR instrument. The collected spectra resulted from 32 scans with a resolution of 4 cm^{-1} over the range of 400–3500 cm^{-1}.

2.2.3. Scanning electron microscopy (SEM)

Scanning electron microscopy (SEM) was used to assess the morphology of BC both before and after crosslinking with PEI. Samples were first mounted on an aluminum SEM stub using carbon tape. Subsequently, they were coated with a 5 nm layer of carbon with the aid of a Leica EM ACE600 sputter coater (Leica Mikrosysteme GmbH, Vienna, Austria). The SEM images were acquired using a high-resolution Regulus 8220 microscope (Hitachi, Ltd., Tokyo, Japan), operated at 1 kV.

2.2.4. Thermogravimetric analysis (TGA)

The thermal degradation of BC and BC-PEI samples was examined by a thermogravimetric analysis instrument (TA Instruments Q-500, US). The weight loss and thermal degradation temperature were recorded in a range of 25 to 700°C with a heating rate of 10°C/min under a nitrogen flow. The 10 wt.% degradation temperature ($T_{d,\ 10\%}$), the 50 wt.% degradation temperature ($T_{d,\ 50\%}$), the first degradation maximum peak ($T_{d,\ max1}$), and the second degradation maximum peak ($T_{d,\ max2}$) were reported.

2.2.5. Differential scanning calorimetry (DSC)

Differential scanning calorimetry was performed using a Q2000 TA Instruments calorimeter employing standard hermetic aluminum pans, calibrated with indium and nitrogen as purge gas. The samples were first cooled from 40 to -90°C at a cooling rate of 10°C/min, and they were analyzed at a heating rate of 10°C/min over a temperature range of -90 to 200°C under a nitrogen atmosphere. The endothermic enthalpies (ΔH_W) showing the water loss from the samples and the temperature associated with it (T_W) are calculated from the heating cycle.

2.3. Antimicrobial Evaluation

2.3.1. Antibacterial tests

The antibacterial test was conducted following ISO 20743:2021 guidelines (Textiles — Determination of the antibacterial activity of textile products) using an absorption method with minor adjustments (ISO, 2021). Two strains of bacteria, *S. aureus* representing gram-positive, and *P. aeruginosa* representing gram-negative, were employed to assess the antibacterial efficacy of BC-PEI. These strains were preserved at −80°C until needed.

To prepare stock cultures, 5 μl of thawed bacteria were inoculated into 5 mL of LB and incubated at 200 rpm, 37°C for 18 h. The bacteria concentration was then adjusted to approximately 3-5 × 10^8 CFU/ml by suitable dilution and by setting OD600 to be equivalent to 1. The stock culture of the bacterial strains was further diluted with nutrient broth (NB) to achieve the final concentrations of 10^6 CFU/ml. The NB was prepared based on the ISO instructions, which involved dissolving 3.0 g of meat extract and 5.0 g of peptone in 1000 ml of Milli-Q water and then adjusting the pH to range between 6.8 and 7.2. Both the unmodified BC (control sample) and the resulting BC-PEI samples were sterilized under a UV lamp for 20 minutes and placed inside sealable vials.

Next, 100 μl of the prepared bacteria inoculum was carefully pipetted onto various points of the sample surface (BC and BC-PEI samples) while ensuring that the pipette did not touch the vial surface. The vials were then incubated at the desired time (1, 2, 4, 6, and 8 h) at 37°C and 90% relative humidity. Three control samples (BC samples) incubated with the bacteria inoculum were also set aside for t=0 h immediately after inoculation.

At the end of the incubation period, 10 ml of the neutralizing solution (D/E Neutralizing Broth solution) was added to the vials containing either the control (BC) or BC-PEI samples. The vials were then thoroughly shaken using a vortex mixer for 5 seconds in 5 cycles. Subsequently, tenfold serial dilutions were created by adding 100 μl of the vortexed mixture into 900 μl of phosphate-buffered saline (PBS) down to 10^4. Finally, the bacterial viability was ascertained by dispersing and incubating 100 μl of the diluted aliquots on solidified agar plates, incubating these plates overnight at 37°C, and enumerating the resultant colony formations.

2.3.2. Antiviral tests

The antiviral test was performed with slight modification following the ISO 18184:2019 protocol entitled "Textiles — Determination of the antiviral activity of textile products" and using the Median Tissue Culture Infectious Dose ($TCID_{50}$) method (ISO, 2019). The human coronavirus 229E (ATCC® VR-740™) and human cell line MRC-5 (ATCC CCL-171™) was used to assess the antiviral activity of the samples. Initially, samples measuring 2×2 cm^2 were sterilized by exposure to UV lamps for 20 minutes. In accordance with ISO 18184:2019 guidelines, essential control tests were conducted to ensure the absence of cytotoxic effects, preservation of cell sensitivity to the virus, and appropriate inactivation of antiviral activity.

For each sample (BC and BC-PEI), 100 μl of virus with a concentration of 3×10^5 $TCID_{50}$/ml was inoculated onto its surface and placed inside a container. Subsequently, the samples were incubated at 25°C for 30 min and 2 h. At the end of the incubation period, the virus was collected by adding 5 ml of the neutralizing solution and vortexing the mixture for 5 seconds in 5 cycles. The obtained solution mixture was serially diluted with EMEM by a factor of 10, resulting in dilutions down to 10^5. From each diluted aliquot, 100 μl was added to a 96-well plate containing MRC-5 cells with a confluency of 50-60% and repeated in quadruple. Following a 1 h incubation at 35°C under 5% CO_2, the virus solution was gently removed, and the cells were washed once with PBS. Finally, the infected cells were incubated in EMEM supplemented with 2% FBS, under the aforementioned conditions, for 96 h until cytopathic effects were observed using a microscope. The $TCID_{50}$ values were calculated using the Spearman–Kärber method.

2.4. Statistical Analysis

The data obtained from the antimicrobial tests were analyzed through the two-way analysis of variance (ANOVA) while using the JMP computer program (JMP® Pro 16.1.0). Tukey's multiple comparison test was considered to be 0.05, in which the p-value <0.05 was interpreted as significant. Since the measurements were repeated in triplicate, the results are presented as mean ± SD.

3. Results and Discussions

The bacterial cellulose explored in this study was synthesized by acetic acid bacteria, notably *Acetobacter xylinum*, through an oxidative fermentation process of a given medium. According to the supplier's data sheet, the resultant BC has a cellulose purity ≥99.9% and a distinctive three-dimensional structure. This structure consists of nanofibers with an approximate diameter of 20 to 50 nm and lengths extending over 10 μm. BC attains a crystallinity of approximately 85-90 % and Young's modulus close to 17 GPa. Having plenty of hydroxyl groups (-OH) in its structure, it can be selectively converted into cellulose derivatives by using various reagents and crosslinkers.

During the crosslinking reaction between BC and PEI, utilizing epichlorohydrin as a crosslinker, an alkaline environment is needed to initiate the reaction. BC is first subjected to epichlorohydrin under alkaline conditions which facilitates the nucleophilic substitution reaction between the hydroxyl groups of BC and the strained epoxide group

of epichlorohydrin (Lin, Gao, Chang, & Ma, 2016). The reactive alkyl halogen end of epichlorohydrin is first linked to the hydroxyl groups of BC, creating a glycidyl ether derivative. Then, the derivative groups covalently couple with the amine groups of PEI (Hermanson, 2013). The reaction pathway is presented in Scheme 1. The selected concentration of epichlorohydrin exhibited no discernible influence on the visual attributes of BC sheets (Fig. S1). Crosslinked BC samples with varying concentrations of PEI, consistently demonstrated comparable transparency, rigidity, and flexibility, with no fragmentation. SEM images, illustrated in Fig. 1, confirm that samples of BC crosslinked with 5 and 10% (wt/v%) PEI retain a similar structural integrity and nanofibers diameter as pristine BC and without any destruction (SEM of samples with 2.5% and 5% (wt/v%) PEI are presented in Fig. S2). Furthermore, the assessment of sample thickness indicated insignificant differences. Accordingly, the thicknesses were measured as: 13.1±1.7 μm for pristine BC, and 13.9±1.1, 13.4±1.6, 12.9±1.8, 13.1±1.4 μm for 2.5%, 5%, 7.5% and 10% (wt/v%) of crosslinked BC-PEI, respectively. However, upon comparison of SEM images, the apparent compaction of the nanofibers in the crosslinked samples is noticeable, potentially caused by an alteration in hydrogen bonding behavior within the crosslinked structure. A previous work by (Pogorelova et al., 2020) documented a similar influence of alkaline treatment and dehydration on the structural characteristics of BC, confirming our observations.

Furthermore, the quantification of crosslinking between PEI and BC matrix was conducted using the colorimetric methodology involving Orange II. Upon analysis, the dye displayed negligible reactivity with pristine BC, while the content of crosslinked PEI was determined as 0.75 ±0.12, 0.89±0.01, 1.16±0.02, and 1.72+0.03 mg/cm^2 in the samples prepared with 2.5%, 5%, 7.5%, and 10% (wt/v%) PEI content, respectively. These findings indicate that an elevation in PEI concentration corresponds directly to an increase in the quantity of crosslinked PEI into BC. This observation proves that although the crosslinker concentration remained constant for all PEI concentrations, it has induced adequate modification while effectively introducing abundant amine

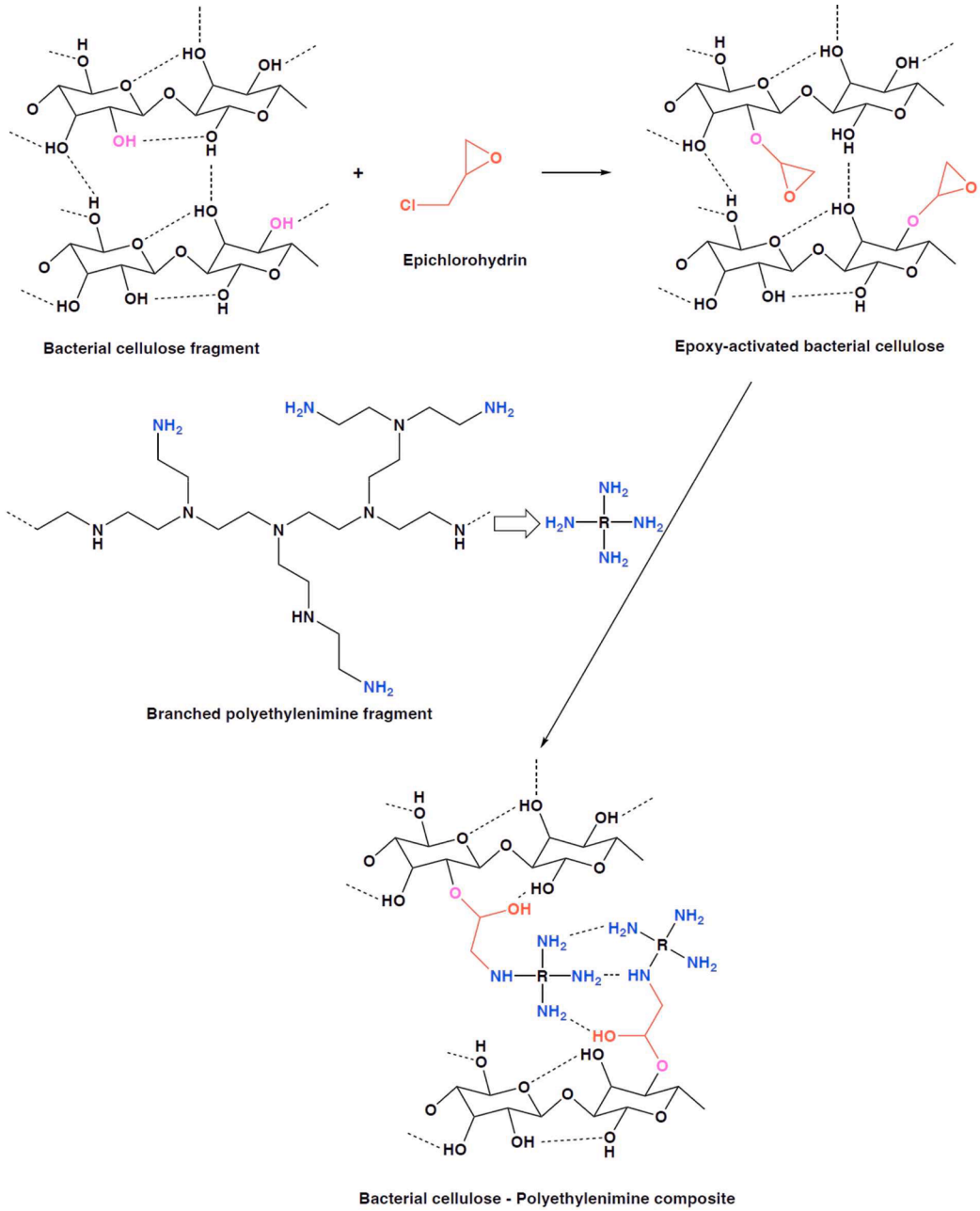

Scheme 1. The reaction pathway of BC crosslinked PEI by using epichlorohydrin under alkaline conditions.

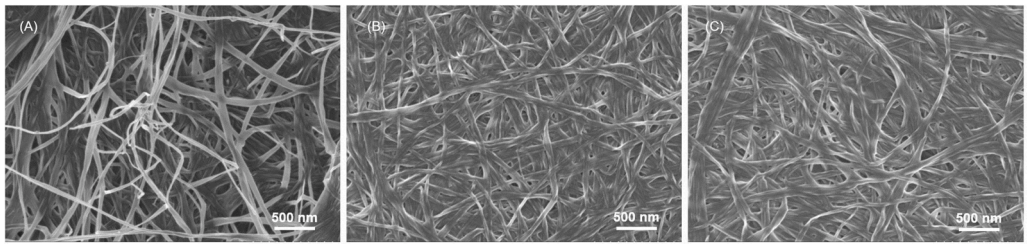

Fig. 1. SEM Images of pristine BC (A), 5% (B) and 10 % (C) PEI crosslinked BC.

functional groups within the BC matrix. As evidenced by SEM analysis, the structural integrity of the BC matrix was preserved without destroying the porous structure.

3.1. TGA Results

To confirm the attachment of PEI onto the matrix of BC, the thermal degradation behavior of the synthesized samples was examined through comprehensive TGA analysis. Fig. 2 presents the TGA and derivative thermogravimetric (DTG) profiles for both pristine BC and BC-PEI samples, featuring varying concentrations of PEI. The DTG curve reveals a marginal weight loss for all samples below 120°C, attributed to the gradual evaporation of loosely absorbed water in the BC matrix. Notably, pure BC displays a primary weight loss peak at approximately 350°C, signifying a complex degradation process involving dehydration, depolymerization, and the cleavage of glycoside bonds. This degradation may lead to the generation of byproducts including CO, CH_4, and water (Jayaramudu, Ko, Zhai, Li, & Kim, 2017). In contrast, PEI demonstrates two distinct weight loss stages, with peak temperatures located at around 318°C and 385°C. These stages correspond to weight losses of approximately 14% and 68%, respectively. Likewise, two degradation stages were also observed in the BC-PEI crosslinked samples, as summarized in Table 1, which are directly related to the modified BC structure with PEI. Indeed, the peak referring to the second degradation stage ($T_{d,\ max2}$) falls around 350°C, which is the primary weight loss peak of BC. However, its values were slightly above 350°C for the BC-PEI crosslinked samples since PEI degrades at a slower rate at temperatures above 350°C, as it can be seen from Fig. 2A. The lowest and highest recorded temperatures of thermal decomposition in the second stage occurred at 351°C and 363°C for samples containing 2.5% and 10% PEI, respectively, as reported in Table 1. These results match the $T_{d,\ 50\%}$ degradation temperatures, which are around 350°C for BC and the modified BC samples.

On the other hand, the BC-PEI crosslinked samples exhibit a first thermal degradation stage ($T_{d,\ max1}$) at temperatures around 280 and 290°C, which is not observed in the neat BC sample. While PEI undergoes a first degradation stage around 300°C, which may result in the appearance of $T_{d,\ max1}$ in the crosslinked samples, the amount of PEI added in this study is small; therefore, the first thermal degradation peak of the BC-PEI samples is caused by other parameters. In fact, the crosslinking of PEI onto BC disrupts some of the strong hydrogen bonding interactions between the hydroxyl groups of the latter and replace them with weaker interactions established between the amine groups of the former with each other and/or the hydroxyl groups of BC, as illustrated in Scheme 1. The weaker interactions leads to a network that is more susceptible to heat degradation, which is probably triggered by the initial thermal degradation of PEI in the crosslinked samples. The $T_{d,\ 10\%}$ degradation temperatures of Table 1 confirm this speculation, as the temperature values decrease by nearly 55°C between neat BC and the crosslinked BC-PEI samples. Besides, a previous study has reported similar phenomena when BC was crosslinked with chitosan (Wahid et al., 2019).

Table 1
Analysis of the TGA and DCS graphs of examined samples.

Samples	$T_{d,\ 10\%}$ (°C)	$T_{d,\ 50\%}$ (°C)	1st stage $T_{d,\ max1}$ (°C)	2nd stage $T_{d,\ max2}$ (°C)	ΔH_W (J/g)	T_W (°C)
PEI	304	377	318	385	-	-
Pristine BC	328	352	-	351	105	84
BC-PEI 2.5%	277	344	287	351	85	69
BC-PEI 5%	272	348	286	360	80	77
BC-PEI 7.5%	273	344	284	355	67	60
BC-PEI 10%	273	350	283	363	85	66

3.2. DSC analysis

The disruption of the strong hydrogen bonding network of the hydroxyl groups found in BC was further confirmed from DSC, and the samples traces are shown in Fig. 3 and reported in Table 1. As observed from the thermogram curves, an endothermic response is evident within the range of 40 to 140°C, which arises from the volatilization of absorbed water molecules by the BC matrix (ΔH_W). The untreated BC

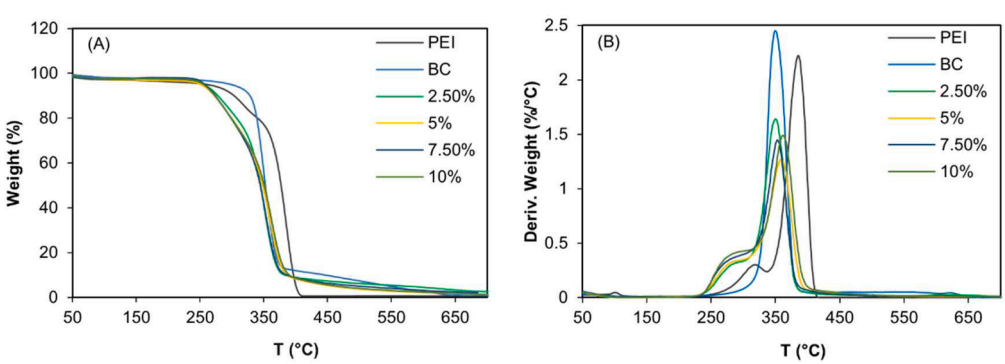

Fig. 2. TGA thermogram (A) and derivative thermogravimetric curve (B) of BC, PEI, and BC crosslinked PEI.

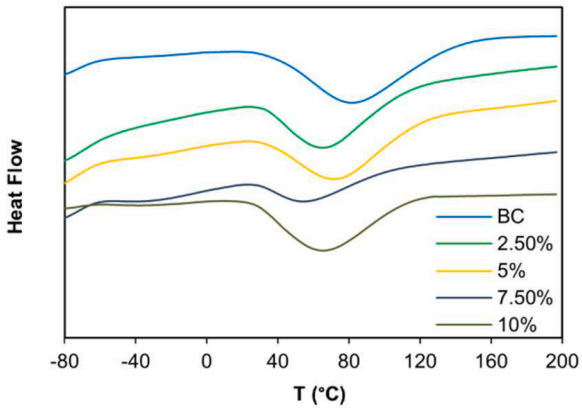

Fig. 3. DSC analysis of pristine BC and BC crosslinked PEI with different concentrations.

specimen manifests a water loss characterized by an enthalpy of 105 J/g, occurring at an endothermic peak (T_W) of 84°C. Upon the introduction of crosslinking and increasing PEI concentrations, a reduction in both enthalpy and temperature becomes discernible in samples containing 2.5%, 5%, and 7.5% (wt/v%) PEI, as summarized in Table 1. Conversely, a marginal enhancement in enthalpy and temperature is observable within samples incorporating 10% (wt/v%) PEI. This phenomenon can be attributed to the crosslinking reaction, which triggers a heightened involvement of hydroxyl groups, subsequently weakening the hydrogen bonding of BC samples with water. With the subsequent addition of PEI, a change in the hydrogen bonding tendency can be observed, owing to the abundance of amine groups and the formation of novel hydrogen bonds between those groups and the hydroxyl groups in BC and water. This observation reinforces the premise that the crosslinking reaction alters the interaction dynamics between the hydroxyl groups of the BC structure and water. Similar effects in ΔH_W and T_W were observed in Oliveira et al.'s study when they chemically modified their BC matrix with methyl groups (Oliveira et al., 2015).

It is worth mentioning that FTIR (Fig. S3) was used as an attempt to detect and quantify the amine-hydroxyl interactions, but they were not detected in the FTIR spectra of the 10% PEI (wt/v%), as the functional groups of BC were dominant. In fact, PEI was added in quantities that could not be probably detected by the instrument.

3.3. Antimicrobial Activity of BC-Crosslinked PEI

3.3.1. Antibacterial efficacy

The antibacterial and antiviral attributes of BC-PEI are pivotal characteristics for their application as advanced antimicrobial masks. In this investigation, the biocidal effectiveness of BC-PEI was assessed using *S. aureus* and *P. aeruginosa*, which represent gram-positive and gram-negative bacterial strains, respectively. Fig. 4 shows a comparative analysis of the antimicrobial efficacy of crosslinked PEI against these bacterial species. In general, results highlight that *P. aeruginosa* displays a lower susceptibility to PEI compared to *S. aureus*, whereas the unmodified BC exhibited negligible impact on both bacterial strains.

Regarding *S. aureus*, all concentrations of crosslinked PEI led to a reduction in viable bacterial colonies. Notably, a 1.5 to 2 log reduction was observed within 1 h of contact time (Fig. 4A). Subsequent increments in either contact time or PEI concentration exerted a substantial influence on diminishing the number of viable colonies. Specifically, after 6 h of contact time, 2.5% PEI concentration completely inhibited *S. aureus* growth, while 10% PEI achieved the same outcome after 2 h. Moreover, exposure times of 4 and 6 h with 5% and 7.5% PEI concentrations resulted in the absence of detectable *S. aureus* colonies. Conversely, *P. aeruginosa* demonstrated greater resilience to PEI treatment. A marginal reduction in bacterial growth was evident for all PEI concentrations during the initial 1 h contact (Fig. 4B). Extending the contact time to 2 h led to a modest decline of 0.5 to 1 logarithmic reduction in bacterial growth. The subsequent prolongation of contact time to 4 h induced further reduction in colony numbers. Remarkably, complete growth inhibition of *P. aeruginosa* was achieved after 6 h of contact with a 7.5% (wt/v%) PEI concentration. This observation aligns with existing research findings, such as those comparing *E. coli* and *S. aureus* (Liu et al., 2018; Wahid et al., 2020). They reported that higher PEI concentrations were generally required to eliminate *E. coli*, which is gram-negative, in comparison to *S. aureus*. This behavior can be attributed to disparities in the membrane structures of gram-positive and gram-negative bacteria. Particularly, gram-positive bacteria, such as *S. aureus,* are surrounded by a thick but porous cell wall, whereas gram-negative bacteria, such as *E. coli* and *P. aeruginosa,* possess an impermeable outer membrane that serves as a barrier to external molecules (Wiegand et al., 2013).

Nevertheless, the established antibacterial mechanism of cationic polymers, such as PEI, primarily involves electrostatic interactions between the numerous positively charged functional groups of the polymer and the negatively charged cell membranes of bacteria. This interaction leads to membrane disruption, causing cytoplasmic leakage and eventual bacterial demise (Wiegand et al., 2013). However, alternate mechanisms, such as induction of cell polarization and increased cell membrane permeability, might contribute to PEI's biocidal action against bacteria, depending on the structure of PEI and its molecular weight (Sahiner, Sagbas, Sahiner, & Ayyala, 2017). For instance, Lin et al. concluded that the hydrophobic polycationic chains effectively traversed the bacterial cellular membrane/wall that induced irreversible damage therein. Furthermore, PEI had to retain its polymeric characteristics, which included the presence of exceptionally long chains, to be effective when immobilized (Lin et al., 2003). Accordingly, the significance of this research lies in demonstrating that branched PEI, even

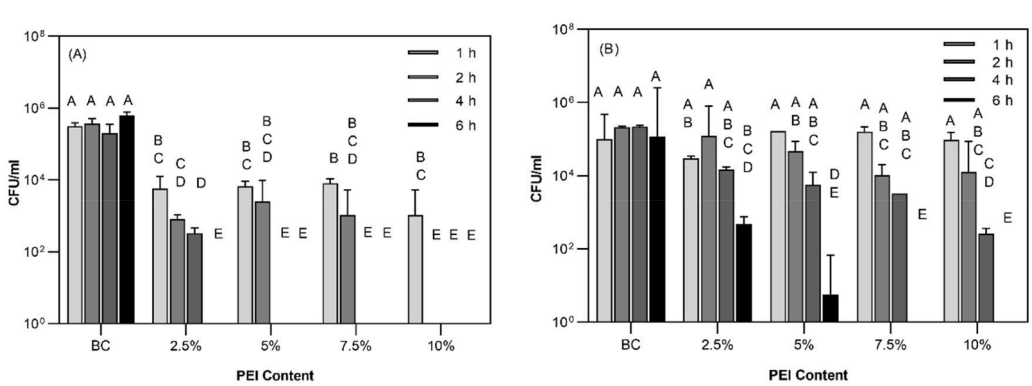

Fig. 4. Antibacterial efficacy of pristine BC and BC crosslinked PEI with various concentrations and contact times against *S. aureus* (A) and *P. aeruginosa* (B). Different letters indicate significantly different groups determined by Tukey's test ($p < 0.05$).

when crosslinked on a BC matrix, retains the capability to either permeate the cell membrane or, owing to its inherent flexibility, encircle bacteria. This allows it to engage in electrostatic interactions, particularly under neutral pH conditions and while being partially moistened.

3.3.2. Antiviral activity

The antiviral effectiveness of the synthesized BC-PEI matrices was assessed using the human coronavirus 229E (HcoV-229E), an enveloped virus that possessed a surface of glycoproteins (Lomartire & Gonçalves, 2022). The outcomes, presented in Fig. 5, depict viral titers after a brief (30 min) and extended (2 h) exposure periods to verify the virucidal efficacy of various PEI contents. Despite the robust biocidal properties exhibited by the BC-PEI samples, their virucidal impact remained moderate as demonstrated in Fig. 5.

It is noteworthy that the complete mechanism by which PEI inhibits viral activity remains incompletely elucidated. Notably, existing research underscores that the antiviral attributes of PEI are not solely dictated by its properties and structural configuration. Wang et al. suggested that the internalization process of Porcine reproductive and respiratory syndrome (PRRS) into the cells might influence the effect of PEI (Wang et al., 2019). They evaluated the virucidal effect of various types of PEI against PRRS. The findings revealed that certain forms of PEI, specifically the linear 25 kDa PEI, effectively inhibited the replication of diverse PRRSV-2 strains in cultured cells, including MARC-145 cells and primary porcine pulmonary alveolar macrophages (PAMs). This inhibition appeared to result from the ability of PEI to obstruct the attachment of PRRSV particles to susceptible cells. Interestingly, PEI had differing effects on PRRSV internalization in different cell types, enhancing internalization in PAMs but having minimal impact on MARC-145 cells (Wang et al., 2019). Also, Spoden et al. findings demonstrated the inhibitory influence of linear PEI on human papillomavirus (HPV) and human cytomegalovirus (HCMV) infections. In fact, preincubating the PEI with cells hindered the primary attachment of both viruses to the cells, resulting in a substantial reduction in infection. Additionally, the repetitive administration of PEI efficiently curtailed the spread of HCMV within cultured cells (Spoden et al., 2012). Larson et al. compared the virucidal activity of PEI and its derivative, N, N-dodecyl,methyl-polyethylenimine (PMPEI), by incubating either one of them with an aqueous solution containing herpes simplex viruses (HSVs) (Larson et al., 2013). The polycationic PMPEI exhibited a modest capacity to decrease the HSV-1 titer by a single logarithmic unit, falling short in comparison to the efficacy of the unalkylated PEI. From these findings, it was deduced that while the polycationic nature played a major role, it was not the exclusive or primary determinant of the anti-HSV activity; a notable degree of hydrophobicity emerged as an additional prerequisite (Larson et al., 2013).

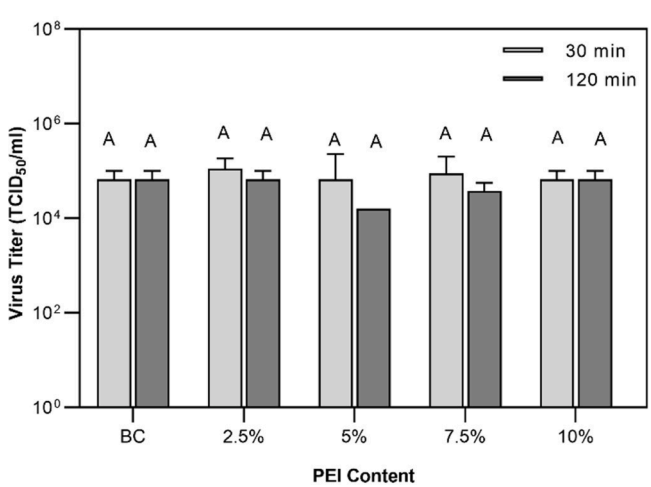

Fig. 5. Antiviral efficacy of BC and BC crosslinked PEI with various concentrations and contact times against HcoV-229E. Different letters indicate significantly different groups determined by Tukey's test ($p < 0.05$).

The precise biocidal mechanism underlying the action of PEI remains partially elucidated. However, its antiviral modus operandi exhibits a heightened level of complexity. While existing research has demonstrated the virucidal effectiveness of both PEI and its derivatives, numerous mechanisms have been postulated to explain their antiviral properties. It is partially understood that PEI might interfere with the virus-cell attachment depending on the type of cell host and virus structure. This hypothesis could explain the relatively week virus inhibition that the BC-PEI samples of this study demonstrated. According to the experimental method, which follows ISO-18184 (ISO, 2019), the virus and the cell were not in contact in the presence of PEI. Indeed, the procedure involved the initial incubation of the virus with the crosslinked samples then the introduction of the treated virus into MRC-5 host cells. Since PEI was attached to BC sheets, it remained in the crosslinked samples after collecting the viruses, and none of it got transferred to the incubation phase of the virus and the cells. As a result, the role of PEI was restricted, as it could not interfere between the cells and the virus to reduce the viral infection. Moreover, the impact of its structural characteristics, such as molecular weight and chain type (linear versus branched), should be considered among other crucial factors that influence its mechanism of action, particularly regarding the virus structure. Consequently, the current findings underscore the need for further investigation, including the exploration of potential divergences in outcomes arising from changes in host cell factors. Additionally, the assessment of the virucidal activity of unbound and free PEI (without immobilization) presents an avenue for discerning potential discrepancies in antiviral effectiveness.

4. Conclusion

This study has successfully demonstrated that dried BC-PEI composites are promising antibacterial porous materials, finding its application as middle filtering layer of face masks. The comprehensive physicochemical characterization revealed that the introduction of PEI through crosslinking did not compromise the structural integrity of BC while decreasing its thermal stability by about 55°C based on $T_{d,\ 10\%}$. Furthermore, the attachment of PEI onto BC disrupted some of the strong hydrogen bonding interactions that exist between the hydroxyl groups of BC. In fact, the amine groups in PEI created weaker hydrogen bonding with each other and with the hydroxyl groups of BC, confirmed by the decrease in ΔH_W and T_W related to water evaporation of the examined samples. Interestingly, the branched PEI significantly enhanced BC susceptibility to gram-positive bacteria, notably *S. aureus*. The rapid inhibition of gram-positive and negative bacterial growths, particularly with PEI concentrations up to 2.5 and 7.5 (wt/v%) within 6 h exposure time, respectively, highlighted the efficacy of BC-PEI composites against such pathogens. However, the antiviral properties of BC-PEI were comparatively limited against human coronavirus 229E (HcoV-229E), suggesting the need for further investigation into the underlying virus inhibition mechanisms, as well as the effect of PEI structure on those mechanisms. This study lays the groundwork for potential advancements in materials science and biomedical applications, offering a unique avenue for the development of antimicrobial materials with diverse uses beyond the scope of this investigation.

CRediT authorship contribution statement

Bentolhoda Heli: Writing – review & editing, Writing – original draft, Visualization, Validation, Software, Project administration, Methodology, Investigation, Formal analysis, Data curation, Conceptualization. **Georges R. Younes:** Writing – review & editing, Validation, Methodology, Formal analysis, Data curation. **Kattin Arguindeguy:** Visualization, Validation, Methodology, Data curation, Conceptualization. **Abdellah Ajji:** Writing – review & editing, Supervision, Resources,

Funding acquisition.

Declaration of competing interest

The authors declare the following financial interests/personal relationships which may be considered as potential competing interests:

Georges R. Younes reports financial support was provided by the Fonds de Recherche du Québec-Nature et Technologie for funding his postdoctoral research under their B3X program. Other authors report financial support was provided by Funding from NSERC discovery grant program and Polytechnique Montréal.

Data availability

Data will be made available on request.

Acknowledgment

Georges R. Younes would like to thank the Fonds de Recherche du Québec-Nature et Techno for funding his postdoctoral research under their B3X program. Funding from NSERC discovery grant program and Polytechnique Montreal are also acknowledged.

Supplementary materials

Supplementary material associated with this article can be found, in the online version, at doi:10.1016/j.carpta.2024.100457.

References

Badshah, M., Ullah, H., Khan, A. R., Khan, S., Park, J. K., & Khan, T. (2018). Surface modification and evaluation of bacterial cellulose for drug delivery. *International Journal of Biological Macromolecules, 113*, 526–533. https://doi.org/10.1016/j.ijbiomac.2018.02.135

Chen, P., Yang, Z., Mai, Z., Huang, Z., Bian, Y., Wu, S., Dong, X., Fu, X., Ko, F., & Zhang, S. (2022). Electrospun nanofibrous membrane with antibacterial and antiviral properties decorated with Myoporum bontioides extract and silver-doped carbon nitride nanoparticles for medical masks application. *Separation Purification Technology, 298*, Article 121565. https://doi.org/10.1016/j.seppur.2022.121565

Gao, C. X., Li, Y., Wei, J., Cotton, S., Hamilton, M., Wang, L., & Cowling, B. J. (2021). Multi-route respiratory infection: When a transmission route may dominate. *Science of The Total Environment, 752*, Article 141856. https://doi.org/10.1016/j.scitotenv.2020.141856

Gope, D., Gope, A., & Gope, P. C. (2020). Mask material: challenges and virucidal properties as an effective solution against coronavirus SARS-CoV-2. *Open Health, 1*(1), 37–50. https://doi.org/10.1515/openhe-2020-0004

Hermanson, G. T. (2013). *Bioconjugate techniques* (3rd ed.). Academic Press-Elsevier Inc. https://doi.org/10.1016/C2009-0-64240-9

ISO. (2019). 18184:2019 Textiles — Determination of antiviral activity of textile products.

ISO. (2021). 20743:2021 Textiles — Determination of antibacterial activity of textile products. In.

Jayaramudu, T., Ko, H.-U., Zhai, L., Li, Y., & Kim, J. (2017). Preparation and characterization of hydrogels from polyvinyl alcohol and cellulose and their electroactive behavior. *Soft Materials, 15*(1), 64–72. https://doi.org/10.1080/1539445X.2016.1246458

Jonsirivilai, B., Torgbo, S., & Sukyai, P. (2022). Multifunctional filter membrane for face mask using bacterial cellulose for highly efficient particulate matter removal. *Cellulose, 29*(11), 6205–6218. https://doi.org/10.1007/s10570-022-04641-3

Kumar, S., Karmacharya, M., Joshi, S. R., Gulenko, O., Park, J., Kim, G.-H., & Cho, Y.-K. (2020). Photoactive antiviral face mask with self-sterilization and reusability. *Nano letters, 21*(1), 337–343. https://doi.org/10.1021/acs.nanolett.0c03725

Lansbury, L., Lim, B., Baskaran, V., & Lim, W. S. (2020). Co-infections in people with COVID-19: a systematic review and meta-analysis. *Journal of Infection, 81*(2), 266–275. https://doi.org/10.1016/j.jinf.2020.05.046

Larson, A. M., Oh, H. S., Knipe, D. M., & Klibanov, A. M. (2013). Decreasing herpes simplex viral infectivity in solution by surface-immobilized and suspended N, N-dodecyl, methyl-polyethylenimine. *Pharmaceutical research, 30*, 25–31. https://doi.org/10.1007/s11095-012-0825-2

Li, Z.-J., Zhang, H.-Y., Ren, L.-L.e.a., & The Chinese Centers for Disease, C., & Prevention Etiology of Respiratory Infection Surveillance Study, T.. (2021). Etiological and epidemiological features of acute respiratory infections in China. *Nature Communications, 12*(1), 5026. https://doi.org/10.1038/s41467-021-25120-6

Lin, J., Qiu, S., Lewis, K., & Klibanov, A. M. (2003). Mechanism of bactericidal and fungicidal activities of textiles covalently modified with alkylated polyethylenimine. *Biotechnology and Bioengineering, 83*(2), 168–172. https://doi.org/10.1002/bit.10651

Lin, Q., Gao, M., Chang, J., & Ma, H. (2016). Adsorption properties of crosslinking carboxymethyl cellulose grafting dimethyldiallylammonium chloride for cationic and anionic dyes. *Carbohydrate Polymers, 151*, 283–294. https://doi.org/10.1016/j.carbpol.2016.05.064

Lin, W.-C., Lien, C.-C., Yeh, H.-J., Yu, C.-M., & Hsu, S.-h. (2013). Bacterial cellulose and bacterial cellulose–chitosan membranes for wound dressing applications. *Carbohydrate Polymers, 94*(1), 603–611. https://doi.org/10.1016/j.carbpol.2013.01.076

Liu, M., Li, J., & Li, B. (2018). Mannose-modificated polyethylenimine: a specific and effective antibacterial agent against Escherichia coli. *Langmuir, 34*(4), 1574–1580. https://doi.org/10.1021/acs.langmuir.7b03556

Liu, Z., Wang, Y., Zu, Y., Fu, Y., Li, N., Guo, N., Liu, R., & Zhang, Y. (2014). Synthesis of polyethylenimine (PEI) functionalized silver nanoparticles by a hydrothermal method and their antibacterial activity study. *Materials Science and Engineering: C, 42*, 31–37. https://doi.org/10.1016/j.msec.2014.05.007

Lomartire, S., & Gonçalves, A. M. M. (2022). Antiviral Activity and Mechanisms of Seaweeds Bioactive Compounds on Enveloped Viruses—A Review. *Marine Drugs, 20*(6), 385. Retrieved from https://www.mdpi.com/1660-3397/20/6/385.

Martins, D., Rocha, C., Dourado, F., & Gama, M. (2021). Bacterial Cellulose-Carboxymethyl Cellulose (BC: CMC) dry formulation as stabilizer and texturizing agent for surfactant-free cosmetic formulations. *J Colloids Surfaces A: Physicochemical Engineering Aspects, 617*, Article 126380. https://doi.org/10.1016/j.colsurfa.2021.126380

Noel, S., Liberelle, B., Yogi, A., Moreno, M. J., Bureau, M. N., Robitaille, L., & De Crescenzo, G. (2013). A non-damaging chemical amination protocol for poly (ethylene terephthalate)–application to the design of functionalized compliant vascular grafts. *Journal of Materials Chemistry B, 1*(2), 230–238. https://doi.org/10.1039/C2TB00082B

Oliveira, R. L., Vieira, J. G., Barud, H. S., Assunção, R., R Filho, G., Ribeiro, S. J., & Messadeqq, Y (2015). Synthesis and characterization of methylcellulose produced from bacterial cellulose under heterogeneous condition. *Journal of the Brazilian Chemical Society, 26*, 1861–1870. https://doi.org/10.5935/0103-5053.20150163

Pandey, A. P., & Sawant, K. K. (2016). Polyethylenimine: A versatile, multifunctional non-viral vector for nucleic acid delivery. *Materials Science and Engineering: C, 68*, 904–918. https://doi.org/10.1016/j.msec.2016.07.066

Pogorelova, N., Rogachev, E., Digel, I., Chernigova, S., & Nardin, D. (2020). Bacterial cellulose nanocomposites: morphology and mechanical properties. *Materials, 13*(12), 2849. https://doi.org/10.3390/ma13122849

Pullangott, G., Kannan, U., Gayathri, S., Kiran, D. V., & Maliyekkal, S. M. (2021). A comprehensive review on antimicrobial face masks: an emerging weapon in fighting pandemics. *RSC advances, 11*(12), 6544–6576. https://doi.org/10.1039/D0RA10009A

Qiu, W.-Z., Zhao, Z.-S., Du, Y., Hu, M.-X., & Xu, Z.-K. (2017). Antimicrobial membrane surfaces via efficient polyethyleneimine immobilization and cationization. *Applied Surface Science, 426*, 972–979. https://doi.org/10.1016/j.apsusc.2017.07.217

Raut, M. P., Asare, E., Syed Mohamed, S. M. D., Amadi, E. N., & Roy, I. (2023). Bacterial Cellulose-Based Blends and Composites: Versatile Biomaterials for Tissue Engineering Applications. *International Journal of Molecular Sciences, 24*(2), 986. https://doi.org/10.3390/ijms24020986

Riva, L., Fiorati, A., & Punta, C. (2021). Synthesis and application of cellulose-polyethyleneimine composites and nanocomposites: A concise review. *Materials, 14*(3), 473. https://doi.org/10.3390/ma14030473

Sahiner, N., Sagbas, S., Sahiner, M., & Ayyala, R. S. (2017). Polyethyleneimine modified poly(Hyaluronic acid) particles with controllable antimicrobial and anticancer effects. *Carbohydrate Polymers, 159*, 29–38. https://doi.org/10.1016/j.carbpol.2016.12.024

Shanmugam, V., Babu, K., Garrison, T. F., Capezza, A. J., Olsson, R. T., Ramakrishna, S., Hedenqvist, M. S., Singha, S., Bartoli, M., & Giorcelli, M. (2021). Potential natural polymer-based nanofibres for the development of facemasks in countering viral outbreaks. *Journal of Applied Polymer Science, 138*(27), 50658. https://doi.org/10.1002/app.50658

Sharma, P., Mittal, M., Yadav, A., & Aggarwal, N. K. (2022). Bacterial cellulose: nano-biomaterial for biodegradable face masks-A greener approach towards environment. *Environmental Nanotechnology, Monitoring Management.* , Article 100759. https://doi.org/10.1016/j.enmm.2022.100759

Spoden, G. A., Besold, K., Krauter, S., Plachter, B., Hanik, N., Kilbinger, A. F., Lambert, C., & Florin, L. (2012). Polyethylenimine is a strong inhibitor of human papillomavirus and cytomegalovirus infection. *Antimicrobial agents and chemotherapy, 56*(1), 75–82. https://doi.org/10.1128/AAC.05147-11

Stanislas, T. T., Bilba, K., de Oliveira Santos, R. P., Onésippe-Potiron, C., Savastano Junior, H., & Arsène, M.-A. (2022). Nanocellulose-based membrane as a potential material for high performance biodegradable aerosol respirators for SARS-CoV-2 prevention: a review. *Cellulose, 29*(15), 8001–8024. https://doi.org/10.1007/s10570-022-04792-3

Wahid, F., Bai, H., Wang, F.-P., Xie, Y.-Y., Zhang, Y.-W., Chu, L.-Q., Jia, S.-R., & Zhong, C. (2020). Facile synthesis of bacterial cellulose and polyethyleneimine based hybrid hydrogels for antibacterial applications. *Cellulose, 27*, 369–383. https://doi.org/10.1007/s10570-019-02806-1

Wahid, F., Hu, X.-H., Chu, L.-Q., Jia, S.-R., Xie, Y.-Y., & Zhong, C. (2019). Development of bacterial cellulose/chitosan based semi-interpenetrating hydrogels with improved mechanical and antibacterial properties. *International Journal of Biological Macromolecules, 122*, 380–387. https://doi.org/10.1016/j.ijbiomac.2018.10.105

Wang, J., Li, J., Wang, N., Ji, Q., Li, M., Nan, Y., Zhou, E.-M., Zhang, Y., & Wu, C. (2019). The 40 kDa Linear Polyethylenimine Inhibits Porcine Reproductive and Respiratory

Syndrome Virus Infection by Blocking Its Attachment to Permissive Cells. *Viruses, 11* (9), 876. Retrieved from https://www.mdpi.com/1999-4915/11/9/876.

Wiegand, C., Bauer, M., Hipler, U.-C., & Fischer, D. (2013). Poly (ethyleneimines) in dermal applications: biocompatibility and antimicrobial effects. *International Journal of Pharmaceutics, 456*(1), 165–174. https://doi.org/10.1016/j.ijpharm.2013.08.001

Wu, A., Hu, X., Ao, H., Chen, Z., Chu, Z., Jiang, T., Deng, X., & Wan, Y. (2022). Rational design of bacterial cellulose-based air filter with antibacterial activity for highly efficient particulate matters removal. *Nano Select, 3*(1), 201–211. https://doi.org/10.1002/nano.202100086

Xiong, S.-W., Fu, P.-g., Zou, Q., Chen, L.-y., Jiang, M.-y., Zhang, P., Wang, Z.-g., Cui, L.-s., Guo, H., & Gai, J.-G. (2020). Heat conduction and antibacterial hexagonal boron nitride/polypropylene nanocomposite fibrous membranes for face masks with long-time wearing performance. *ACS applied materials & interfaces, 13*(1), 196–206. https://doi.org/10.1021/acsami.0c17800

Zhang, J., Han, Y., Ben, Z., Han, T., & Yin, P. (2023). Effect of branched polyethyleneimine and citric acid on the structural, physical and antibacterial properties of corn starch/chitosan films. *International Journal of Biological Macromolecules, 231*, Article 123186. https://doi.org/10.1016/j.ijbiomac.2023.123186

Żywicka, A., Ciecholewska-Juśko, D., Charęza, M., Drozd, R., Sobolewski, P., Junka, A., Gorgieva, S., El Fray, M., & Fijałkowski, K. (2023). Argon plasma-modified bacterial cellulose filters for protection against respiratory pathogens. *Carbohydrate Polymers, 302*, Article 120322. https://doi.org/10.1016/j.carbpol.2022.120322